TYPE Mini Review
PUBLISHED 14 November 2022
DOI 10.3389/fbuil.2022.1048533

OPEN ACCESS

EDITED BY
Yongjia Xu,
Tsinghua University, China

REVIEWED BY
Gabriele Milani,
Politecnico di Milano, Italy
Biagio Carboni,
Sapienza University of Rome, Italy
Lili Hu,
Shanghai Jiao Tong University, China

*CORRESPONDENCE
Raffaele Capuano,
raffaele.capuano@unina.it

SPECIALTY SECTION
This article was submitted to Earthquake Engineering,
a section of the journal
Frontiers in Built Environment

RECEIVED 19 September 2022
ACCEPTED 26 October 2022
PUBLISHED 14 November 2022

CITATION
Capuano R, Fraddosio A and Piccioni MD (2022), Phenomenological rate-independent uniaxial hysteretic models: A mini-review.
Front. Built Environ. 8:1048533.
doi: 10.3389/fbuil.2022.1048533

Phenomenological rate-independent uniaxial hysteretic models: A mini-review

Raffaele Capuano[1]*, Aguinaldo Fraddosio[2] and Mario Daniele Piccioni[2]

[1]Department of Structures for Engineering and Architecture, University of Naples Federico II, Napoli, Italy, [2]Department of Civil Engineering Sciences and Architecture, Polytechnic University of Bari, Bari, Italy

A great variety of phenomenological models has been proposed over the years to model rate-independent hysteretic forces in structural mechanics. The classification of such models is usually based on the type of equation that needs to be solved to evaluate the output variable. In particular, we distinguish among algebraic, transcendental, differential and integral models. For algebraic (transcendental) models, an algebraic (a transcendental) equation needs to be solved to compute the output variable; conversely, differential equations are employed for differential models, whereas equations expressed in integral form characterize integral models. This paper provides a mini-review of the most adopted phenomenological rate-independent uniaxial hysteretic models. Such models are selected in order to provide a complete overview of the four types of previously mentioned models, currently available in the literature. In particular, we illustrate the fundamental characteristics of each model and discuss their peculiarities in terms of 1) number of adopted parameters and variables, 2) physical interpretation of parameters and related calibration procedures, 3) type of hysteresis loop shapes that can be simulated.

KEYWORDS

phenomenological models, hysteresis, structural dynamics, structural mechanics, structural engineering

1 Introduction

The mathematical modeling of hysteresis phenomena is a challenging problem addressed during the years by different authors by means of different models. The main aim of the various authors was to obtain accurate and computationally efficient models based on a small number of parameters (Vaiana et al., 2019b). The model proposed in the literature can be classified into four main categories based on the type of equation that need to be solved to compute the output variable (Vaiana et al., 2018; Vaiana et al., 2021b). In particular, we have: 1) algebraic, 2) transcendental, 3) differential, 4) integral models.

2 Algebraic models

2.1 Ramberg-Osgood model

The Ramberg-Osgood model is an algebraic model formulated by Ramberg and Osgood (1943). In this model, generally used for simulating the behavior of steel, the generalized displacement u is assumed as the output variable and is expressed as the sum of two terms:

$$u = u_e + u_p, \tag{1}$$

an elastic and a plastic generalized displacement indicated, respectively, as u_e and u_p. In particular, the generalized displacement is evaluated in a closed-form as:

$$u = \frac{f}{E} + K\left(\frac{f}{E}\right)^n, \tag{2}$$

where E is the elastic modulus, K and n are constants that depend on the considered material. The first term on the right-hand side of Eq. 2 is equal to the elastic part of the generalized displacement, whereas the second term accounts for the plastic part. The parameters K and n describe the hardening behavior of the material. Introducing the generalized yield force of the material f_y, and defining a new parameter α as:

$$\alpha = K\left(\frac{f}{E}\right)^{n-1}, \tag{3}$$

it is possible to rewrite the general expression as follows:

$$u = \frac{f}{E} + \alpha\frac{f}{E}\left(\frac{f}{f_y}\right)^{n-1}. \tag{4}$$

Since Eq. 4 defines the skeleton curve, it is necessary to adopt the Masing rule (Masing and Mauksch, 1926) in order to simulate an entire hysteresis loop.

2.2 Giuffrè-Menegotto-Pinto model

As reported in Carreño et al. (2020), the model was first developed by Giuffrè (1970), and was based on the nonlinear stress-strain relation proposed by Goldberg and Richard (1963) and incorporates the effect of plastic deformations on the Bauschinger effect observed in steel tested experimentally. The formulation was further improved by Menegotto and Pinto (1973) and subsequently used by multiple authors due to its simplicity and accuracy in predicting the response of reinforcing steel. Filippou et al. (1983) later incorporated the effect of isotropic hardening into the constitutive law. The formulation proposed by Filippou is often preferred in the modeling of reinforced concrete systems given the consistent response and limited failures in convergence observed in the nonlinear analysis of large structural models. The constitutive relation of the model is:

$$f = \left[E_h + \frac{E - E_h}{\left(1 + \left|\frac{u}{u_y}\right|^r\right)^{\frac{1}{r}}}\right]u, \tag{5}$$

where E is the elastic modulus, E_h is the post-elastic stiffness, u_y is the yield generalized displacement and r is a parameter which controls the rate of variation of the tangent stiffness from E to E_h. In particular, the expression for the evaluation of the parameter r is:

$$r = r_0 - \frac{a_1\frac{u}{u_y}}{a_2 + \frac{u}{u_y}}. \tag{6}$$

Since Eq. 5 defines the skeleton curve, as done for the Ramberg-Osgood model, it is necessary to adopt the Masing rule in order to simulate an entire hysteresis loop.

2.3 Algebraic model

The model proposed by Vaiana et al. (2019a) is a uniaxial phenomenological model which can simulate hysteresis loops limited by two parallel straight lines or curves by adopting a set of only five parameters easy to calibrate (Sessa et al., 2020). Furthermore, the model allows one to evaluate the output variable by means of a closed form expression having an algebraic nature.

In particular, the generalized force f, during the generic loading phase $(\dot{u} > 0)$, can be evaluated as:

$$f\left(u, u_j^+\right) = \begin{cases} c^+\left(u, u_j^+\right) & \text{if} \quad u < u_j^+ \\ c_u(u) & \text{if} \quad u > u_j^+, \end{cases} \tag{7}$$

whereas, during the generic unloading phase $(\dot{u} < 0)$, it can be computed as:

$$f\left(u, u_j^-\right) = \begin{cases} c^-\left(u, u_j^-\right) & \text{if} \quad u > u_j^- \\ c_l(u) & \text{if} \quad u < u_j^-. \end{cases} \tag{8}$$

In Eqs. 7 and 8, c^+ and c^- represent, respectively, the generic loading and unloading curves whose expressions are:

$$c^+\left(u, u_j^+\right) = \beta_1 u^3 + \beta_2 u^5 + k_b u + f_0 + \frac{k_a - k_b}{1 - \alpha}\left[\left(1 + u - u_j^+ + 2u_0\right)^{1-\alpha} - (1 + 2u_0)^{1-\alpha}\right], \tag{9}$$

$$c^-\left(u, u_j^-\right) = \beta_1 u^3 + \beta_2 u^5 + k_b u - f_0 + \frac{k_a - k_b}{\alpha - 1}\left[\left(1 - u + u_j^- + 2u_0\right)^{1-\alpha} - (1 + 2u_0)^{1-\alpha}\right], \tag{10}$$

whereas c_u and c_l are, respectively, the upper and lower limiting curves having expressions:

$$c_u(u) = \beta_1 u^3 + \beta_2 u^5 + k_b u + f_0, \tag{11}$$

$$c_l(u) = \beta_1 u^3 + \beta_2 u^5 + k_b u - f_0. \tag{12}$$

The internal variable u_j^+ (u_j^-), characterizing the generic loading (unloading) phase, is given by:

$$u_j^+ = 1 + u_P + 2u_0 - \left\{ \frac{1-\alpha}{k_a - k_b} \left[f_P - \beta_1 u_P^3 - \beta_2 u_P^5 - k_b u_P - f_0 \right.\right.$$
$$\left.\left. + (k_a - k_b) \frac{(1+2u_0)^{1-\alpha}}{1-\alpha} \right] \right\}^{\frac{1}{1-\alpha}}, \tag{13}$$

$$u_j^- = -1 + u_P - 2u_0 + \left\{ \frac{\alpha-1}{k_a - k_b} \left[f_P - \beta_1 u_P^3 - \beta_2 u_P^5 - k_b u_P + f_0 \right.\right.$$
$$\left.\left. + (k_a - k_b) \frac{(1+2u_0)^{1-\alpha}}{\alpha-1} \right] \right\}^{\frac{1}{1-\alpha}}, \tag{14}$$

where u_P and f_P are the coordinates of the initial point of c^+ (c^-).

The internal model parameters u_0 and f_0 can be expressed in terms of the parameters k_a, k_b, and α as follows:

$$u_0 = \frac{1}{2}\left[\left(\frac{k_a - k_b}{\delta_k} \right)^{\frac{1}{\alpha}} - 1 \right], \tag{15}$$

$$f_0 = \frac{k_a - k_b}{2(1-\alpha)} \left[(1+2u_0)^{1-\alpha} - 1 \right], \tag{16}$$

where δ_k is the difference between the two different values assumed by the transverse tangent stiffness at u_j^+ (u_j^-). However, the authors suggests, based on the results of several numerical tests (Vaiana et al., 2020; Vaiana et al., 2021a; Pellecchia et al., 2022), to set $\delta_k = 10^{-20}$.

3 Transcendental models

3.1 Kikuchi-Aiken model

The transcendental model proposed by Kikuchi and Aiken (1997) was formulated with the purpose of accurately predicting the response of elastomeric bearings (Losanno et al., 2019; Losanno et al., 2022a; Losanno et al., 2022b; Losanno et al., 2022c).

The generalized force f is expressed as the sum of two terms:

$$f(u) = f_1(u) + f_2(u), \tag{17}$$

where

$$f_1(u) = \frac{1}{2}\left(1 - \frac{f_u}{f_m}\right) f_m \left[u + \operatorname{sgn}(u)|u|^n \right], \tag{18}$$

and

$$f_2(u) = \begin{cases} f_u\left\{1 - 2e^{-a\left(1+\frac{u}{u_m}\right)} + b\left(1+\frac{u}{u_m}\right)e^{-c\left(1+\frac{u}{u_m}\right)}\right\} & \text{if} \quad \dot{u} > 0 \\ -f_u\left\{1 - 2e^{-a\left(1-\frac{u}{u_m}\right)} + b\left(1-\frac{u}{u_m}\right)e^{-c\left(1-\frac{u}{u_m}\right)}\right\} & \text{if} \quad \dot{u} < 0. \end{cases} \tag{19}$$

In particular, f_u is the generalized force at zero generalized displacements, f_m is the generalized peak force on the skeleton curve, u_m is the generalized peak displacement on the skeleton curve and the parameter n specifies the stiffening phenomenon. The model parameters a, b, and c are obtained by imposing the following expressions:

$$\frac{1-e^{-2a}}{a} = 1 - \frac{\pi h_{eq} f_m}{2 f_u}, \tag{20}$$

$$b = c^2 \left\{ \frac{\pi h_{eq} f_m}{f_u} - \left[2 + \frac{2}{a}\left(e^{-2a} - 1\right) \right] \right\}, \tag{21}$$

where h_{eq} is the equivalent viscous damping ratio, evaluated from an empirical formula as a function of the generalized force, which is determined from the results of tests performed on individual bearings. Both Eqs. 20 and 21 are derived assuming that the analytical hysteresis loop area matches the experimental one.

Eq. 19 are derived for application to steady-state hysteresis behaviors for elastomeric bearings. Masing rule is applied to fully define the generalized force under a randomly-varying displacement, and Eq. 19 are replaced by:

$$f_2(u) = \begin{cases} f_{2i} + f_u\left\{2 - 2e^{-a\left(\frac{u-u_i}{u_m}\right)} + b\left(\frac{u-u_i}{u_m}\right)e^{-c\left(\frac{u-u_i}{u_m}\right)}\right\} & \text{if} \quad \dot{u} > 0 \\ f_{2i} - f_u\left\{2 - 2e^{a\left(\frac{u-u_i}{u_m}\right)} - b\left(\frac{u-u_i}{u_m}\right)e^{c\left(\frac{u-u_i}{u_m}\right)}\right\} & \text{if} \quad \dot{u} < 0, \end{cases} \tag{22}$$

where

$$f_{2i} = f_i - f_1, \tag{23}$$

and (u_i, f_i) is the most recent point of load reversal.

3.2 Vaiana-Rosati model

The model proposed by Vaiana and Rosati (2023) is a new uniaxial phenomenological model which can simulate a great number of rate-independent hysteretic responses characterized by symmetric, asymmetric, pinched, S-shaped, flag-shaped hysteresis loops or by a combination of them. The model is based on two sets of eight parameters controlling the loading and unloading phase in a separate way. Furthermore, the model allows one to evaluate the output variable by means of a closed form expression having an exponential nature.

In particular, the generalized force f, during the generic loading phase $(\dot{u} > 0)$, can be evaluated as:

$$f\left(u, u_j^+\right) = \begin{cases} c^+\left(u, u_j^+\right) & \text{if} \quad u < u_j^+ \\ c_u(u) & \text{if} \quad u > u_j^+, \end{cases} \tag{24}$$

whereas, during the generic unloading phase $(\dot{u} < 0)$, it can be computed as:

$$f\left(u, u_j^-\right) = \begin{cases} c^-\left(u, u_j^-\right) & \text{if} \quad u > u_j^- \\ c_l(u) & \text{if} \quad u < u_j^-. \end{cases} \tag{25}$$

In Eqs. 24 and 25, c^+ and c^- represent, respectively, the generic loading and unloading curves whose expressions are:

$$c^+\left(u,u_j^+\right)=\beta_1^+e^{\beta_2^+u}-\beta_1^++\frac{4\gamma_1^+}{1+e^{-\gamma_2^+\left(u-\gamma_3^+\right)}}-2\gamma_1^++k_b^+u+f_0^+ -\frac{1}{\alpha^+}\left[e^{-\alpha^+\left(+u-u_j^++\bar{u}^+\right)}-e^{-\alpha^+\bar{u}^+}\right], \quad (26)$$

$$c^-\left(u,u_j^-\right)=\beta_1^-e^{\beta_2^-u}-\beta_1^-+\frac{4\gamma_1^-}{1+e^{-\gamma_2^-\left(u-\gamma_3^-\right)}}-2\gamma_1^-+k_b^-u-f_0^- +\frac{1}{\alpha^-}\left[e^{-\alpha^-\left(-u+u_j^-+\bar{u}^-\right)}-e^{-\alpha^-\bar{u}^-}\right], \quad (27)$$

whereas c_u and c_l are, respectively, the upper and lower limiting curves having expressions:

$$c_u(u)=\beta_1^+e^{\beta_2^+u}-\beta_1^++\frac{4\gamma_1^+}{1+e^{-\gamma_2^+\left(u-\gamma_3^+\right)}}-2\gamma_1^++k_b^+u+f_0^+, \quad (28)$$

$$c_l(u)=\beta_1^-e^{\beta_2^-u}-\beta_1^-+\frac{4\gamma_1^-}{1+e^{-\gamma_2^-\left(u-\gamma_3^-\right)}}-2\gamma_1^-+k_b^-u-f_0^-. \quad (29)$$

The internal variable u_j^+ (u_j^-), characterizing the generic loading (unloading) phase, is given by:

$$u_j^+=u_P+\bar{u}^++\frac{1}{\alpha^+}\ln\left\{+\alpha^+\left[\beta_1^+e^{\beta_2^+u_P}-\beta_1^++\frac{4\gamma_1^+}{1+e^{-\gamma_2^+\left(u_P-\gamma_3^+\right)}}-2\gamma_1^+ +k_b^+u_P+f_0^++\frac{1}{\alpha^+}e^{-\alpha^+\bar{u}^+}-f_P\right]\right\}, \quad (30)$$

$$u_j^-=u_P-\bar{u}^--\frac{1}{\alpha^-}\ln\left\{-\alpha^-\left[\beta_1^-e^{\beta_2^-u_P}-\beta_1^-+\frac{4\gamma_1^-}{1+e^{-\gamma_2^-\left(u_P-\gamma_3^-\right)}}-2\gamma_1^- +k_b^-u_P-f_0^--\frac{1}{\alpha^-}e^{-\alpha^-\bar{u}^-}-f_P\right]\right\}, \quad (31)$$

where u_P and f_P are the coordinates of the initial point of c^+ (c^-).

4 Differential models

4.1 Bouc-Wen model

The Bouc-Wen model is a uniaxial rate-independent hysteretic model, having a differential nature, that has been originally formulated by Bouc (1967) and subsequently extended by Wen (1976). The model is capable of simulating symmetric generalized force-displacement hysteresis loops (Visintin, 2013; Carboni et al., 2018). In the formulation of the model proposed by Wen (1980), the differential equation that defines the model and that needs to be solved is:

$$\dot{f}=-\beta\dot{u}\left|f\right|^n-\gamma\left|\dot{u}\right|\left|f\right|^{n-1}f+A\dot{u}, \quad (32)$$

where β, γ, A and n influence the generalized force-displacement hysteresis loop shape. In particular, parameters γ and β control the shape of the hysteresis loop, A the restoring force amplitude, and n the rate of variation between the initial and the asymptotic tangent stiffness, a large value of n corresponds to an almost bilinear hysteresis loop.

4.2 Ozdemir model

The model was proposed by Ozdemir (1976) and illustrated in more detail in Graesser and Cozzarelli (1991). The model proposed by Ozdemir is a modified form of the Bouc-Wen model. This model is general enough to include a variety of different types of hysteretic behavior. In addition, the material model is linked to experimental studies of the properties of a nickel-titanium shape-memory alloy (SMA). The equations that describe the model are:

$$\begin{cases}\dot{f} &= E\left[\dot{u}-\left|\dot{u}\right|\left(\frac{f-\beta}{Y}\right)^n\right]\\ \dot{\beta} &= \alpha E\left|\dot{u}\right|\left(\frac{f-\beta}{Y}\right)^n,\end{cases} \quad (33)$$

TABLE 1 Uniaxial phenomenological models.

type	model	n° of parameters	internal variables	loops shapes
Algebraic	Ramberg-Osgood	4	3	(A)
	Giuffrè-Menegotto-Pinto	6	3	(A)
	Algebraic	5	4	(A), (E)
Transcendental	Kikuchi-Aiken	5	5	(A), (C), (E)
	Vaiana-Rosati	16	4	(A)–(H)
Differential	Bouc-Wen	4	-	(A)
	Ozdemir	4	1	(A), (G)
Integral	Preisach	$\mu(\alpha, \beta)$	-	(I)

10.3389/fbuil.2022.1048533

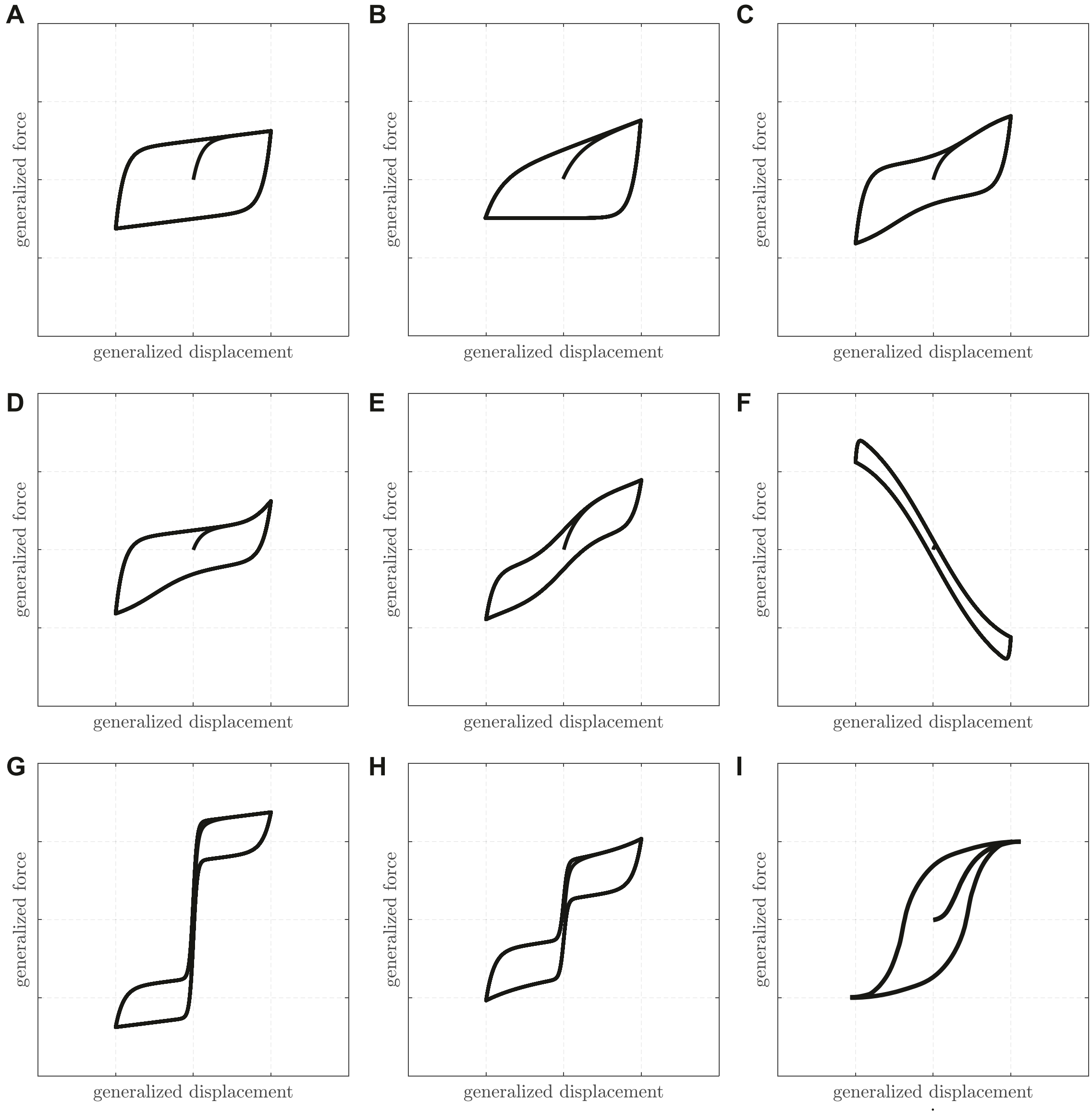

FIGURE 1
Hysteresis loops shapes.

where f is the generalized force, u is the generalized displacement, β is the generalized back-force, E is the elastic modulus, Y is the generalized force correspondent to the point obtained as the intersection of the upper limiting straight line and the tangent line to the origin, n is a constant parameter controlling the rate of variation of the tangent stiffness from E to the asymptotic value E_y, and α is a constant controlling the tangent stiffness of the hysteresis loop and is given by:

$$\alpha = \frac{E_y}{E - E_y}. \quad (34)$$

5 Integral models

5.1 Preisach model

The Preisach model, first derived in Preisach (1935) and than described in Kuczmann (2010) and Mayergoyz (1986), is an integral model given by:

$$f(t) = \iint_{\alpha \geq \beta} \mu(\alpha, \beta)\, \gamma(\alpha, \beta, u(t))\, d\alpha d\beta. \quad (35)$$

The model is obtained considering an infinite set of simplest hysteresis operators γ. These operators can be represented by rectangular loops on the input-output plane. Numbers α and β correspond to up and down switching values of input. The outputs of these operators may assume only two values, + 1 and −1.

Along with the set of operators γ, the model considers an arbitrary weight function $\mu(\alpha, \beta)$. To determine $\mu(\alpha, \beta)$, the set of first order reversal curves should be experimentally found. This can be done by bringing first the input to such a value that outputs of all operators γ are equal to −1. Now if we gradually increase the input value, then we will follow along a limiting ascending branch. The notation f_α will be used for the output value on this branch corresponding to the input $u = \alpha$. The notation $f_{\alpha\beta}$ will be used for the output value on the transition curve attached to the limiting ascending branch at the point f_α. This output value corresponds to the input $u = \beta$. At this point we can define the function:

$$F(\alpha, \beta) = \frac{f_\alpha - f_{\alpha\beta}}{2}. \tag{36}$$

Finally it can be proved that:

$$\mu(\alpha, \beta) = \frac{\partial^2 F(\alpha, \beta)}{\partial\alpha\partial\beta}. \tag{37}$$

6 Discussion

In this review, we made an overview of some celebrated and recently formulated models to illustrate their fundamental characteristics with particular attention to the number of parameters that need to be set (Table 1) and, if present, their physical interpretation. We also show the different kinds of hysteresis loop shapes, shown in Figure 1, that can be simulated by using the different models.

In particular, from Table 1 it can be noted that:

- differential models require a small number of parameters but can simulate only simple hysteresis loops shape;
- models such as the algebraic Ramberg-Osgood, the Giuffrè-Menegotto-Pinto, and the transcendental Kikuchi-Aiken, define only the skeleton curve of a loop. Therefore, it is necessary to use the Masing rule to simulate an entire hysteresis loop, which involves the addition of a series of internal variables;
- the Vaiana-Rosati model, despite the number of parameters, allows for the simulation of the vast majority of hysteresis loop shapes through closed-form expressions;
- the hysteresis loop shape in Figure 1I, typical of the magnetic hysteresis, can be simulated only by the Preisach model, which presents significant difficulties in the evaluation of the output variable.

Author contributions

RC: Writing—original draft, Writing—review and editing. AF: Supervision. MP: Supervision.

Conflict of interest

The authors declare that the research was conducted in the absence of any commercial or financial relationships that could be construed as a potential conflict of interest.

The reviewer GM declared a past co-authorship with the authors AF, MP to the handling editor.

Publisher's note

References

Bouc, R. (1967). "Forced vibration of mechanical systems with hysteresis," in Proceedings of the 4th Conference on Nonlinear Oscillation, Prague, Czechoslovakia, September 5–9, 1967.

Carboni, B., Lacarbonara, W., Brewick, P. T., and Masri, S. F. (2018). Dynamical response identification of a class of nonlinear hysteretic systems. *J. Intelligent Material Syst. Struct.* 29, 2795–2810. doi:10.1177/1045389x18778792

Carreño, R., Lotfizadeh, K., Conte, J., and Restrepo, J. (2020). Material model parameters for the giuffrè-menegotto-pinto uniaxial steel stress-strain model. *J. Struct. Eng. (N. Y. N. Y).* 146, 04019205. doi:10.1061/(asce)st.1943-541x.0002505

Filippou, F. C., Popov, E. P., and Bertero, V. V. (1983). *Effects of bond deterioration on hysteretic behavior of reinforced concrete joints.* EERC Report 83/19, Berkeley: Earthquake Engineering Research Center, University of California.

Giuffrè, A. (1970). Il comportamento del cemento armato per sollecitazioni cicliche di forte intensità. *G. del Genio Civ.* 28, 1–20.

Goldberg, J. E., and Richard, R. M. (1963). Analysis of nonlinear structures. *J. Struct. Div.* 89, 333–351. doi:10.1061/jsdeag.0000948

Graesser, E., and Cozzarelli, F. (1991). Shape-memory alloys as new materials for aseismic isolation. *J. Eng. Mech.* 117, 2590–2608. doi:10.1061/(asce)0733-9399(1991)117:11(2590)

Kikuchi, M., and Aiken, I. D. (1997). An analytical hysteresis model for elastomeric seismic isolation bearings. *Earthq. Eng. Struct. Dyn.* 26, 215–231. doi:10.1002/(sici)1096-9845(199702)26:2<215:aid-eqe640>3.0.co;2-9

Kuczmann, M. (2010). Dynamic preisach hysteresis model. *J. Adv. Res. Phys.* 1.

Losanno, D., Hadad, H., and Serino, G. (2019). Design charts for eurocode-based design of elastomeric seismic isolation systems. *Soil Dyn. Earthq. Eng.* 119, 488–498. doi:10.1016/j.soildyn.2017.12.017

Losanno, D., Calabrese, A., Madera-Sierra, I., Spizzuoco, M., Marulanda, J., Thomson, P., et al. (2022a). Recycled versus natural-rubber fiber-reinforced bearings for base isolation: review of the experimental findings. *J. Earthq. Eng.* 26, 1921–1940. doi:10.1080/13632469.2020.1748764

Losanno, D., De Domenico, D., and Madera-Sierra, I. (2022b). Experimental testing of full-scale fiber reinforced elastomeric isolators (freis) in unbounded configuration. *Eng. Struct.* 260, 114234. doi:10.1016/j.engstruct.2022.114234

Losanno, D., Palumbo, F., Calabrese, A., Barrasso, T., and Vaiana, N. (2022c). Preliminary investigation of aging effects on recycled rubber fiber reinforced bearings (rr-frbs). *J. Earthq. Eng.* 26, 5407–5424. doi:10.1080/13632469.2021.1871683

Masing, G., and Mauksch, W. (1926). "Über das verhalten von kalt gerecktem messing bei zug-und stauchbelastung," in *Wissenschaftliche Veröffentlichungen aus dem Siemens-Konzern* (Springer), 142–155.

Mayergoyz, I. (1986). Mathematical models of hysteresis. *IEEE Trans. Magn.* 22, 603–608. doi:10.1109/tmag.1986.1064347

Menegotto, M., and Pinto, P. (1973). "Method of analysis for cyclically loaded r. c. plane frames including changes in geometry and non-elastic behavior of elements under combined normal force and bending," in Proc.of IABSE Symposium on Resistance and Ultimate Deformability of Structures Acted on by Well Defined Repeated Loads, Lisbona, 15–22.

Ozdemir, H. (1976). *Nonlinear transient dynamic analysis of yielding structures*. Berkeley: University of California.

Pellecchia, D., Lo Feudo, S., Vaiana, N., Dion, J.-L., and Rosati, L. (2022). A procedure to model and design elastomeric-based isolation systems for the seismic protection of rocking art objects. *Comput. aided. Civ. Eng.* 37, 1298–1315. doi:10.1111/mice.12775

Preisach, F. (1935). Über die magnetische nachwirkung. *Z. Phys.* 94, 277–302. doi:10.1007/bf01349418

Ramberg, W., and Osgood, W. R. (1943). Description of stress-strain curves by three parameters. Tech. rep.

Sessa, S., Vaiana, N., Paradiso, M., and Rosati, L. (2020). An inverse identification strategy for the mechanical parameters of a phenomenological hysteretic constitutive model. *Mech. Syst. Signal Process.* 139, 106622. doi:10.1016/j.ymssp.2020.106622

Vaiana, N., and Rosati, L. (2023). Classification and unified phenomenological modeling of complex uniaxial rate-independent hysteretic responses. *Mech. Syst. Signal Process.* 182, 109539. doi:10.1016/j.ymssp.2022.109539

Vaiana, N., Sessa, S., Marmo, F., and Rosati, L. (2018). A class of uniaxial phenomenological models for simulating hysteretic phenomena in rate-independent mechanical systems and materials. *Nonlinear Dyn.* 93, 1647–1669. doi:10.1007/s11071-018-4282-2

Vaiana, N., Sessa, S., Marmo, F., and Rosati, L. (2019a). An accurate and computationally efficient uniaxial phenomenological model for steel and fiber reinforced elastomeric bearings. *Compos. Struct.* 211, 196–212. doi:10.1016/j.compstruct.2018.12.017

Vaiana, N., Sessa, S., Paradiso, M., Marmo, F., and Rosati, L. (2019b). "An efficient computational strategy for nonlinear time history analysis of seismically base-isolated structures," in Conference of the Italian association of theoretical and applied Mechanics (Springer), 1340–1353. doi:10.1007/978-3-030-41057-5_108

Vaiana, N., Marmo, F., Sessa, S., and Rosati, L. (2020). "Modeling of the hysteretic behavior of wire rope isolators using a novel rate-independent model," in *Nonlinear dynamics of structures, systems and devices* (Springer), 309–317. doi:10.1007/978-3-030-34713-0_31

Vaiana, N., Capuano, R., Sessa, S., Marmo, F., and Rosati, L. (2021a). Nonlinear dynamic analysis of seismically base-isolated structures by a novel opensees hysteretic material model. *Appl. Sci.* 11, 900. doi:10.3390/app11030900

Vaiana, N., Sessa, S., and Rosati, L. (2021b). A generalized class of uniaxial rate-independent models for simulating asymmetric mechanical hysteresis phenomena. *Mech. Syst. Signal Process.* 146, 106984. doi:10.1016/j.ymssp.2020.106984

Visintin, A. (2013). *Differential models of hysteresis*, 111. Berlin, Heidelberg: Springer Science & Business Media.

Wen, Y.-K. (1976). Method for random vibration of hysteretic systems. *J. Engrg. Mech. Div.* 102, 249–263. doi:10.1061/jmcea3.0002106

Wen, Y. (1980). Equivalent linearization for hysteretic systems under random excitation. *J. Appl. Mech.* 47, 150–154. doi:10.1115/1.3153594